Advances in Science and Technology Research Journal

Advances in Science and Technology Research Journal, 2027, 21(1), 334–349
https://doi.org/10.12913/22998624/235866
ISSN 2299-8624, License CC-BY 4.0

Received: 2026.08.11
Accepted: 2026.11.15
Published: 2026.12.01

Analysis of the potential for modifying selected combustion parameters of rapeseed oil–n-hexane blends in a diesel engine by varying the angle of the first pilot injection

Dawid Tatarynow[1]

[1] Department of Automotive Engineering, Faculty of Mechanical Engineering, Lublin University of Technology, ul. Nadbystrzycka 38, Lublin, Poland
E-mail: d.tatarynow@pollub.pl

ABSTRACT

Requirements and regulations concerning the increased share of fuels derived from renewable sources are continually becoming more stringent. This constitutes an important motivation for research into alternative fuels applicable in compression-ignition engines. No studies isolating the effect of the first pilot injection (P1) timing angle alone on the combustion course of a rapeseed oil–n-hexane blend have so far been found in the literature. The aim of the study was a preliminary assessment of the effect of varying the start-of-injection angle of P1 on the combustion characteristics of a rapeseed oil blend containing 10% n-hexane (OR90Hex10). Particular attention was paid to isolating the effect of P1 alone on the combustion course. Tests were performed on a chassis dynamometer with a Fiat Qubo 1.3 Multijet (Euro 5), ECU maps modified via WinOLS, at 50 km/h with a load torque of 50 Nm. The start-of-injection angle of P1 was varied in the range from −4 to +4 °CA relative to the nominal setting (°CA – crank angle degree). Settings of the second pilot injection and main injection remained unchanged. Each of the presented results was averaged over n = 100 engine operating cycles**.** The highest indicated pressure (pi = 0.999 MPa) occurred under nominal control; advancing P1 increased dp/dα and Qmax, retarding it reduced them. A retardation of +2 °CA constituted a compromise solution. It reduced the maximum rate of pressure rise dp/dα by approximately 7.7% relative to the nominal injection-angle setting for OR90Hex10 (from 0.594 to 0.548 MPa/°CA). This was accompanied by a reduction in pi of 2.6–4.7% – from 0.999 MPa to the range of 0.952–0.973 MPa, obtained for injection-angle retardation corrections from +1 to +4 °CA. The angle of maximum combustion pressure for the rapeseed oil–n-hexane blend, on the other hand, was α p max = 11.40 °CA, 0.07 °CA less than diesel fuel's 11.33 °CA. The preliminary results indicate that adjusting the timing angle of P1 may constitute a useful calibration parameter for limiting the rate of combustion pressure rise in rapeseed oil–n-hexane blends; confirming this requires research over a broader range of engine operating points.

Keywords: ECU remapping, common rail, rapeseed oil, pilot injection timing.

INTRODUCTION

The increasingly stringent requirements regarding exhaust gas toxic emissions, including the Euro 5 and Euro 6 standards and the proposed Euro 7 requirements [1, 2], constitute an important impetus for the search for alternative energy sources for compression-ignition engines. At the same time, Directive (EU) 2018/2001 of the European Parliament and of the Council on the promotion of the use of energy from renewable sources [3], together with its 2023 amendment [4], sets out the directions for increasing the share of renewable fuels in transport. In this context, rapeseed oil and its derivatives constitute an important group of first-generation alternative fuels [5, 6].

Among the available feedstocks, rapeseed oil is a particularly promising alternative fuel under Central European conditions – in Poland alone, the

rapeseed sown area amounted to approximately 1.0 million ha in 2024, with an average yield of approximately 3240 kg/ha and a harvest of approximately 3.3 million tons [7]. Favorable climatic and soil conditions enable the cultivation of both winter and spring rapeseed, ensuring a stable feedstock supply regardless of seasonal fluctuations.

The primary limitation to the direct use of rapeseed oil as a fuel for compression-ignition engines is its high viscosity, many times greater than that of diesel fuel [8, 9]. Misra and Murthy [8] reported that the viscosity of vegetable oils can be 10–12 times higher than that of diesel fuel, directly affecting the pumping, atomization, and metering of fuel by the injection system. Nwafor and Rice [10] demonstrated that using rapeseed oil blends in a diesel engine results in a prolonged ignition delay and changes in the progression of the individual combustion phases. The authors also emphasized the need to adapt the injection advance angle to the ignition properties of the given alternative fuel. Labecki et al. [11] found that the combustion of rapeseed oil blends can reduce NOx emissions while increasing soot emissions compared with diesel fuel. Yoshimoto and Tamaki [12], in turn, demonstrated that rapeseed oil–diesel fuel blends in equal volumetric proportions can provide energy parameters close to those obtained with conventional diesel fuel supply.

One way to reduce the unfavorable physicochemical properties of rapeseed oil is to modify it using viscosity-reducing additives. Longwic, Sander et al. [13, 14] demonstrated that adding 10% n-hexane to rapeseed oil results in more than a threefold reduction in viscosity, while bringing the density and surface tension closer to those characteristic of diesel fuel. Subsequent studies [15] confirmed the feasibility of operating a compression-ignition engine equipped with a common-rail injection system when fuelled with a rapeseed oil–n-hexane blend, without the need to introduce significant design modifications. Jaworski et al. [16] assessed the self-ignition properties of rapeseed oil–n-hexane blends in a constant-volume combustion chamber and a compression-ignition engine, confirming the feasibility of their use in common-rail fuel systems. The most recent studies [17], meanwhile, showed that a rapeseed oil blend with a 10% addition of n-hexane, when kept in contact with ethanol, yields the highest torque and power values among the analyzed rapeseed oil-based fuels.

The choice of a 10% n-hexane concentration as a component of the tested blend is based on empirical evidence: a 5% by volume addition of n-hexane did not eliminate the starting difficulties observed when an engine warmed up to operating temperature and was fuelled with rapeseed oil. Only a 10% addition of n-hexane permanently removed this problem. Among the tested concentrations of 10% and 15%, both yielded the most favorable energy- and emission-related engine parameters; however, the blend containing 10% n-hexane (OR90Hex10) was selected for further research owing to its lower share of the volatile component and correspondingly more favorable operational properties [15].

Despite the favorable effect of n-hexane on the physicochemical properties of rapeseed oil, the OR90Hex10 blend shows significant differences relative to diesel fuel, which determine the course of the combustion process in a compression-ignition engine with a common-rail injection system. The kinematic viscosity of OR90Hex10 at 40 °C is 19.64 mm²/s and is approximately 7 times higher than the viscosity of diesel fuel (2.7 mm²/s) [13, 14]. Such a high viscosity increases hydraulic flow resistance in the injection system, worsens fuel atomization quality, and increases the diameter of the droplets formed, thereby prolonging the physical phase of combustible-mixture preparation. The surface tension of OR90Hex10 at 20 °C is 30.08 mN/m, slightly higher than that of diesel fuel (29.15 mN/m), thereby affecting droplet formation parameters at the injector outlet [13]. The cetane number of OR90Hex10 is 44.7, compared with 51.2 for diesel fuel [16], indicating a lower propensity of the blend towards self-ignition. The density of OR90Hex10 at 15 °C is 895 kg/m³, compared with approximately 840 kg/m³ for diesel fuel − under nominal ECU control calibrated for diesel fuel, the volumetric dose of OR90Hex10 delivers a different amount of chemical energy per engine cycle. The combined effect of the aforementioned differences in physicochemical properties, under nominal injection-system control, manifests itself as a shift of the start-of-combustion angle of the OR90Hex10 blend towards earlier crankshaft rotation angles compared with diesel fuel, which leads to a higher maximum rate of pressure rise dp/dα and an earlier angular position of the maximum combustion pressure α_{pmax} [15]. This phenomenon results from a different course of the physical phase of combustible-mixture preparation, primarily

related to the fuel's fractional composition and flash point – n-hexane has a flash point of −22 °C, which promotes early evaporation and ignition of the blend's light fraction.

In modern compression-ignition engines equipped with accumulator-type (common-rail) injection systems, what matters is not only the selection of the fuel's physicochemical properties but also the ability to modify the injection-process control parameters [18, 19]. Li, Backes, and Wachtmeister [20] demonstrated that increasing the rail fuel pressure and advancing the start of the main injection intensifies the combustion process of rapeseed oil preheated to 55 °C. Teoh et al. [21] demonstrated that the start-of-injection angle affects exhaust emissions and engine operating parameters in biodiesel-fueled engines. Bo, Wu et al. [22], meanwhile, showed that a multi-phase injection strategy significantly affects the ignition and combustion process, especially under low-temperature conditions.

Current research confirms that the proper selection of the injection angle is one of the fundamental directions for adapting compression-ignition engines to fuelling with bio-component fuels. Fayad [23] analyzed the effect of the fuel injection-angle strategy on performance, combustion course, toxic-emission levels, and particulate-matter characteristics when the engine was fueled with rapeseed oil methyl esters. He showed that an earlier injection of B100 fuel causes a slight increase in in-cylinder pressure and heat release rate compared with diesel fuel. Vallejo et al. [24] demonstrated that an appropriate correction of the injection advance angle, combined with the selection of nozzle geometry, allows the operating parameters of an engine fueled with rapeseed oil to be brought closer to those obtained when fueled with diesel. Sethin et al. [25], studying the effect of diesel–biodiesel blends on exhaust emissions in a common-rail direct-injection engine, indicated that in the ECU remapping process, favorable engine operating settings were achieved by increasing the fuel pressure and changing the injector operating range. Singh et al. [26] analyzed the selection of injection angle and injection pressure in a multi-cylinder common-rail direct-injection engine fuelled with a biodiesel blend. Gowrishankar and Krishnasamy [27], meanwhile, carried out a CFD analysis of the combustion and emission process for biodiesel under conventional injection conditions and a late-injection combustion strategy.

The importance of adapting the injection-system control strategy to the properties of plant-based fuels is also confirmed by studies conducted directly on rapeseed oil and its blends. Vojtisek-Lom, Pechout, and Mazac [28] indicated that engines equipped with common-rail systems require adjustments to the control strategy, including modifications to the injection angle, to ensure proper combustion of plant-based fuels. Yoon et al. [29], studying rapeseed oil–diesel fuel blends in proportions of 10/90, 20/80, and 30/70, observed an increase in combustion pressure with an increasing share of rapeseed oil in the fuel. Turkcan [30], analyzing three-component blends with bioethanol addition, confirmed that a two-phase injection strategy can mitigate the adverse effects of fuelling an engine with alternative fuels. Bambuleac [31] analyzed the injection process of rapeseed oil and rapeseed oil methyl ester in a common-rail engine, demonstrating a delay in rapeseed oil injection compared with diesel fuel.

The literature review presented above shows that modifying the start-of-injection angle is an effective means of shaping the combustion process in rapeseed oil–n-hexane blends. The mechanism of this effect arises from the role of the pilot injection in a multi-phase injection strategy. The pilot dose serves as preliminary thermal and chemical conditioning of the cylinder charge − it initiates local oxidation reactions, raising the local temperature, thereby shortening the ignition delay of the main dose. A change in the start-of-injection angle of the first pilot injection modifies this process relative to top dead center (TDC). Retarding P1 causes charge conditioning to occur closer to TDC and at a higher compressed-air pressure, which shifts the start-of-combustion angle towards later crankshaft rotation angles. As a consequence, the share of kinetic (premixed) combustion decreases, thereby reducing the maximum rate of pressure rise, $dp/d\alpha$, and the maximum heat release rate, Q_{max}. The angle at which the maximum combustion pressure $\alpha_{p\ max}$ occurs shifts towards values characteristic of diesel fuel. Advancing P1 produces the opposite effect − earlier charge conditioning increases the share of the kinetic combustion phase, intensifying the pressure rise. The start-of-injection angle of P1, therefore, serves as a regulatory parameter for shaping combustion dynamics, rather than the energy dose, making it a suitable tool for correcting the combustion course of the OR90Hex10 blend without design modifications to the fuel supply system.

Despite numerous studies on the use of rapeseed oil and its blends as alternative fuels [32–36], the literature still lacks in-depth analyses of how changes in injection-system control parameters affect the combustion process of rapeseed oil–n-hexane blends. Previous studies have focused primarily on selecting blend compositions and assessing basic engine energy- and emission-related parameters. Comparatively little attention, on the other hand, has been paid to the possibility of using the regulation of individual injection phases, particularly the first pilot injection, as a tool for shaping the combustion course of such a fuel in an engine equipped with a common-rail system.

The novelty of the present study lies in the experimental isolation of the effect of the first pilot injection (P1) alone on the indicated combustion parameters of the rapeseed oil–n-hexane blend (OR90Hex10). Studies [13–17] focused on the selection of composition and the physicochemical properties of this blend. Studies [20, 23, 24, 26], in turn, analyzed the effect of the injection angle on other bio-derived fuels − preheated rapeseed oil, rapeseed oil methyl esters, and biodiesel blends. No studies isolating the effect of changing the angle of the first pilot injection alone for the OR90Hex10 blend have been found in the available literature.

The aim of the present study is a preliminary assessment of the possibility of modifying selected combustion parameters of a rapeseed oil blend with a 10% n-hexane addition by changing the start-of-injection angle of the first pilot injection (P1). This correction is intended to serve as a tool for shaping the combustion course without design modifications to the fuel supply system.

A research hypothesis was formulated that a modification of the start-of-injection angle of the first pilot injection (P1) affects the combustion dynamics of the OR90Hex10 blend (as expressed by the parameters $dp/d\alpha$ and Q_{max}) more strongly than it affects its energy parameters (as expressed by the parameter p_i).

Driving conditions at 50 km/h with a load torque of 50 Nm were selected as the test point. An analysis of the injection control phases showed the presence of all three injection phases − P1, P2, and G − precisely at this engine load level. Modifying only the P1 angle, with the P2 and G settings unchanged, made it possible to unambiguously attribute the observed changes in combustion parameters to the effect of the first pilot injection.

MATERIALS AND METHODS

Test stand and research objects

The subject of the study was a compression-ignition engine equipped with a common-rail fuel injection system, installed in a Fiat Qubo 1.3 Multijet vehicle. The tested vehicle met the Euro 5 exhaust emission standard and was equipped with a five-speed manual gearbox. The engine's technical data are presented in Table 1, while a view of the test vehicle is shown in Figure 1.

The vehicle was fitted with an AVL INDIMICRO 602 engine indicating system with a built-in signal amplifier, supporting four analog input channels and two digital inputs, allowing the real-time recording of fast-changing parameters. The signals recorded by the AVL IndiMicro system were:

- in-cylinder pressure trace: recorded by means of an AVL GH13P piezoelectric sensor mounted in the glow-plug seat of the first cylinder, whose signal was processed in the amplifier − AVL measurement module. According to the manufacturer's data sheet (AVL List GmbH, Pressure Sensor for Combustion Analysis – Data Sheet GH13P, no. TIGG0931A.01), this sensor is characterised by: a measuring range of 0–250 bar, linearity ≤±0.3% FSO (≤±0.75 bar over the full range), a nominal sensitivity of 16 pC/bar, a permissible overload of 300 bar, a natural frequency of approximately 130 kHz, an operating temperature range of −40 to 400 °C, a drift under cyclic temperature changes of ≤±0.5 bar, and a thermal shock error of ≤±0.3 bar (corresponding to ≤±1.5% for IMEP and ≤±1% for maximum pressure, according to the manufacturer's data);
- crankshaft position signal: information on the crankshaft position was obtained from an inductive sensor cooperating with the toothed flywheel via an AVL Universal Pulse Conditioner 389Z01 analog-to-digital converter. An AVL 389/303 – Inductive encoder configuration with a 60–2 marker disc was used, for which − thanks to internal signal interpolation − an angular resolution of 0.1 °CA was obtained; acquisition of the measurement signals was carried out synchronously with the crankshaft rotation angle (rather than at a fixed time frequency), in accordance with the architecture of the AVL IndiMicro system;

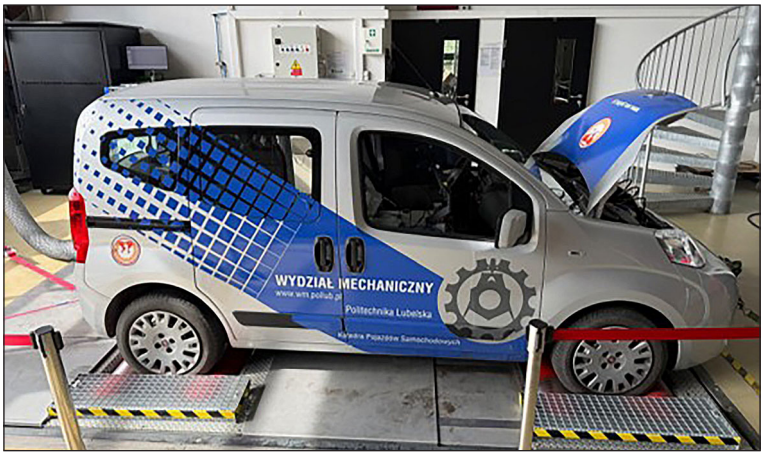


Figure 1. View of the test vehicle Fiat Qubo 1.3 Multijet

Table 1. Technical data of the 1.3 Multijet engine of the Fiat Qubo test vehicle

Parameter	Value
Displacement	1248 cm³
Cylinder bore	69.6 mm
Piston stroke	82 mm
Compression ratio	16.8 : 1
Maximum power	55 kW / 75 hp
Maximum torque	190 Nm
Idle speed	850 ± 20 RPM
Speed at maximum torque	1500 RPM
Fuel injection system	Common rail
Exhaust aftertreatment	Exhaust gas recirculation, diesel particulate filter

- injection parameters: analyzed on the basis of the analog control signal of the electromagnetic injector, after conversion to a digital signal. The actual injector opening moment recorded in this way differs from the value programmed in the ECU control unit map – this difference results from the injector's electromagnetic and hydraulic delays. For this reason, throughout the remainder of the paper, we consistently use the measured value (e.g., the angle α_{pw}) rather than the setting programmed in the control unit.

Two fuels were used in the study: diesel fuel as the reference fuel, and a blend of rapeseed oil with a 10% addition of n-hexane, designated OR90Hex10. The blend was prepared in a volumetric ratio of 90% rapeseed oil and 10% n-hexane. The vegetable oil used was refined rapeseed oil, marketed under the trade name "Olej Kujawski" by Zakłady Tłuszczowe "Kruszwica" S.A. in Kruszwica. The n-hexane was supplied by Avantor Performance Materials Poland S.A., based in Gliwice. The addition of 10% n-hexane to rapeseed oil reduces the fuel density at 15 °C from approximately 916 kg/m³ to approximately 895 kg/m³, corresponding to a decrease of approximately 2–3%. At the same time, the kinematic viscosity at 40 °C decreases from 34.89 mm²/s to 19.64 mm²/s, i.e., by approximately 56%. The cetane number of the OR90Hex10 blend is 44.7, compared with 45.2 for pure rapeseed oil. The heat of combustion of pure rapeseed oil and n-hexane, determined by the same authors for the same fuel system [15], is 35,284.32 kJ/dm³ and 31,911 kJ/dm³, respectively; for blends in the 0–20% n-hexane range, the heat of combustion decreases slightly with an increasing n-hexane share, from 35,284.32 to 34,609.66 kJ/dm³ [15]. Interpolating linearly between these values (own calculation, not stated directly in [15]), an approximate value of about 34,947 kJ/dm³ is obtained for the OR90Hex10 blend (10% n-hexane). A summary of the basic physicochemical properties of the test fuels is presented in Table 2.

The tests were carried out on a DF4FS-HLS chassis dynamometer, enabling the simulation of real-world vehicle driving conditions. The dynamometer was equipped with DynoRace software, used for test-bench control and measurement data acquisition. The technical data of the chassis dynamometer are summarised in Table 3.

Modifications to the ECU control software were carried out using a dedicated bench for reading, writing, and programming the control maps. The bench comprised a Magic Motorsport FLEX MASTER device, a Fronius Acctiva

Table 2. Physicochemical properties of the test fuels

Property	Diesel fuel	Rapeseed oil	RO + 10% n-hexane
Density at 15 °C (kg/m³)	~835	~916	~895
Kinematic viscosity at 40 °C (mm²/s)	2–4.5	34.89	19.64
Cetane number	>51	45.2	44.7

Professional Flash 70A power supply, WinOLS software version 4.51, a mobile computer with the Flex and WinOLS software installed, and a copy of the Fiat Qubo vehicle's ECU. The control maps for the fuel injection process were identified using the WinOLS software. The maps selected for further modification were those defining the injection angle, expressed in degrees of crankshaft rotation, as a function of the fuel dose delivered (mm³/cycle) and the engine crankshaft rotational speed.

Course of test

In the first stage of the study, an analysis of the fuel injection phases was conducted under nominal engine control conditions. The purpose of this part was to determine which injection phases − i.e., the first pilot injection (P1), the second pilot injection (P2), and the main injection (G) (the adopted designations were used consistently throughout the paper) − are executed by the ECU at the operating points corresponding to the conditions of the subsequent indicated-parameter measurements. The tests at this stage were conducted with the engine fueled with diesel fuel.

The analysis was carried out over a crankshaft rotational speed range of 1500 to 4000 rpm, with the speed varied in 500 rpm increments. Measurements were conducted for three load states: the load resulting solely from rolling resistance in driving-simulation mode, an applied braking torque of 40 Nm, and an applied braking torque of 60 Nm. The injection control signals were recorded as a function of the engine crankshaft rotation angle at each operating point. This made it possible to unambiguously determine the presence and angular positions of the first, second, and main pilot injections. Under the load resulting solely from rolling resistance, the first pilot injection did not occur at any of the tested operating points in the 1500–4000 rpm range. Under these conditions, the ECU executed only the second pilot injection and the main injection.

Table 3. Technical data of the DF4FS-HLS chassis dynamometer

Parameter	Value
Maximum axle load	2500 kg
Maximum speed	300 km/h
Maximum power (accelerating axle)	400 kW
Maximum power (continuously loaded axle)	300 kW
Tractive force	7500 N
Accuracy of power and torque measurement	±2%

At a braking force of 40 Nm, the second pilot injection and the main injection occurred over the entire analyzed speed range. The first pilot injection, on the other hand, appeared selectively, depending on engine speed. At 1500 rpm, the first pilot injection was recorded in the range from -36 to -33 °CA, the second pilot injection in the range from -7 to −5 °CA, and the main injection in the range from -2 to +7 °CA. At 2000 rpm, the first pilot injection did not occur; the second pilot injection was executed in the range from -22 to -17 °CA, and the main injection from +1 to +7 °CA. At 2500 rpm, the first pilot injection was recorded from −31 to −27 °CA and the main injection from -4 to +4 °CA. At 3000 rpm, the second pilot injection occurred in the range from -31 to -27 °CA, and the main injection from -8 to +2 °CA. At 3500 rpm, the second pilot injection occurred from -34 to -30 °CA, and the main injection from -9 to +1 °CA. At 4000 rpm, the ECU executed only the main injection over the range of -12 to +2 °CA, while the pilot injections were disabled.

At a braking force of 60 Nm, the control strategy was three-pulse in the lower-speed range, with the first pilot injection maintained over 1500–2000 rpm. At 1500 rpm, the first pilot injection occurred in the range from -36 to -33 °CA, the second pilot injection from -10 to -7 °CA, and the main injection from +2 to +4 °CA. At 2000 rpm, the first pilot injection was executed from -30 to -27 °CA, the second pilot injection from -12 to -9 °CA, and the main injection from -2 to +4 °CA. At 2500 rpm, the second pilot injection

was recorded from −32 to −28 °CA and the main injection from -5 to +5 °CA. At 3000 rpm, the second pilot injection occurred from -35 to -31 °CA, and the main injection from −8 to +2 °CA. At 3500 rpm, the second pilot injection occurred from -34 to -30 °CA, and the main injection from −10 to +3 °CA. The measurement at 4000 rpm and a load of 60 Nm was not performed because the engine did not reach this rotational speed at the specified load value (Figure 2).

Based on the analysis, the first pilot injection is optional, and its frequency increases with engine load. The second pilot injection and the main injection were executed at most of the analyzed operating points. As rotational speed and fuel dose increased, their duration, expressed in degrees of crankshaft rotation, became shorter. In the upper speed range, the ECU simplified the injection strategy, limiting it to the main injection executed near TDC.

50 km/h and an applied load of 50 Nm. These conditions were selected owing to the confirmed first pilot injection at the established engine operating point. Within this range, it was possible to assess the effect of changing the P1 start-of-injection angle on the indicated and dynamic combustion parameters of the OR90Hex10 blend, while maintaining the nominal settings of the second pilot injection P2 and the main injection G. Each of the presented indicated-parameter results was averaged over n = 100 engine operating cycles, recorded for the established operating point.

The recorded indicator traces were quantitatively analyzed in the AVL IndiCom environment using the computational algorithms implemented in the software. The mathematical relationships presented, as well as the values of the parameter κ − the polytropic exponent − were adopted in accordance with the AVL IndiCom technical

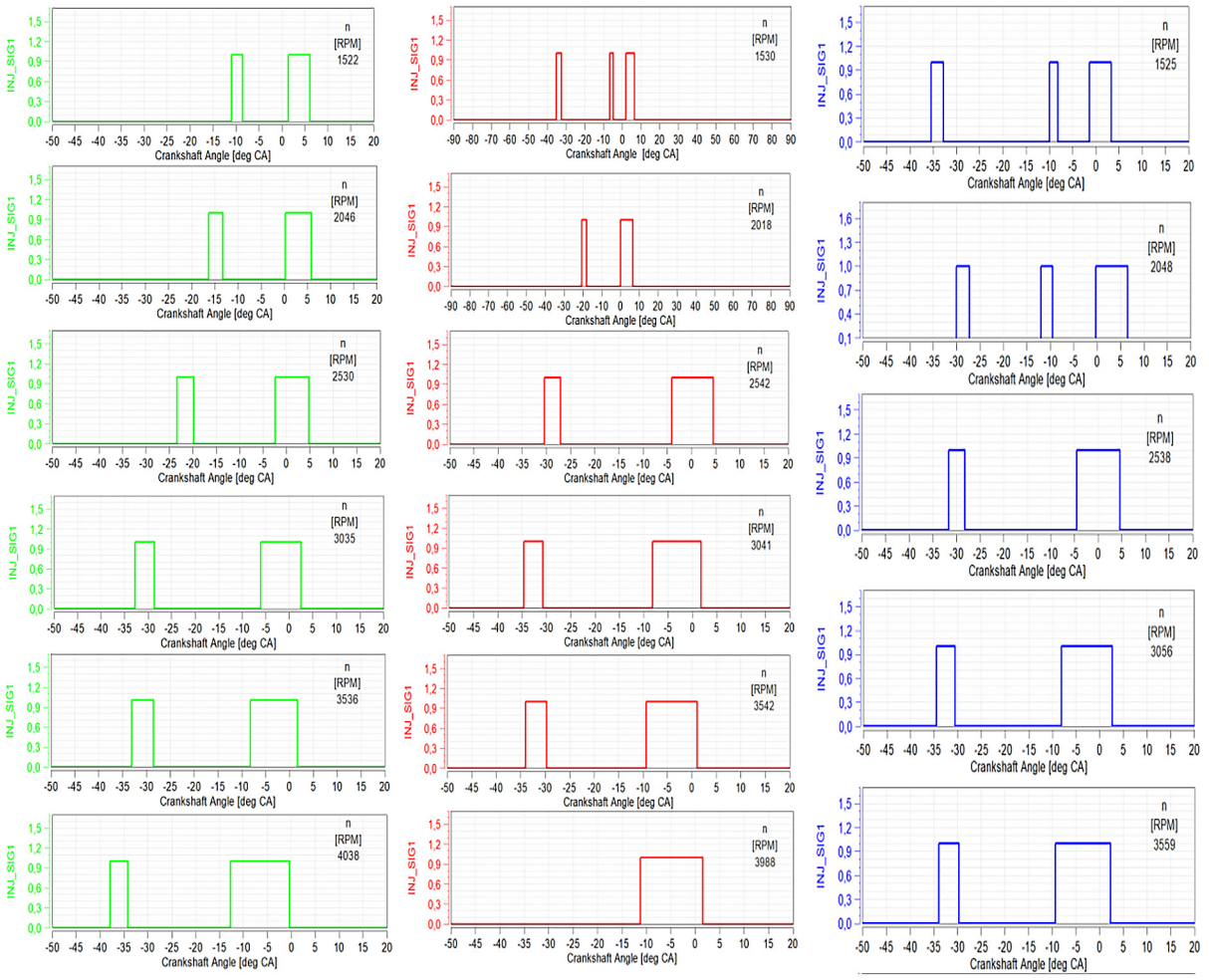


Figure 2. Diesel fuel injection control phases during driving on the chassis dynamometer: green − with the load resulting from driving resistance; red − with an applied braking torque of 40 Nm; blue − with an applied braking torque of 60 Nm, at rotational speeds increased in steps of 500 rpm from 1500 to 4000 rpm, as a function of the engine crankshaft rotation angle

documentation and the measurement-project configuration used during the tests.
The mean indicated pressure was determined as

$$p_i = (1/V_{ss}) \cdot \oint p \, dV \quad (1)$$

where: p – instantaneous in-cylinder pressure, V – instantaneous cylinder volume as a function of crankshaft rotation angle, V_{ss} – displacement volume.

The maximum combustion pressure was determined as

$$p_{max} = max[p(\theta)] \quad (2)$$

and the corresponding angle at which the maximum in-cylinder pressure occurs was determined as the value of the argument of the function p(θ) for which the pressure reaches its maximum within the analyzed crankshaft rotation angle interval,

$$\alpha_{p\,max} = argmax[p(\theta)] \quad (3)$$

The maximum rate of pressure rise dp/dα was determined as the highest value of the pressure difference quotient with respect to crankshaft rotation angle within a single operating cycle. The energy quantities given in the further part of the paper in units of kJ/m³ (mean amount of fuel dose burned, Figure 6 and kJ/(m³·°CA) (Q_{max}, Figure 7) are, analogously to pi, referenced to the same cylinder displacement volume V_{ss}. The heat release rate was calculated by the AVL IndiCom software according to a simplified model based on the first law of thermodynamics:

$$Q_i = [C/(\kappa - 1)] \cdot [\kappa \cdot p_i \cdot (V_i + n - V_i - n) + V_i \cdot (p_i + n - p_i - n)] \quad (4)$$

where: n denotes the calculation step (1 °CA), κ – the polytropic exponent (κ = 1.37 for the compression phase and κ = 1.30 for the expansion phase – values adopted in the AVL IndiCom measurement-project configuration), and C – the unit conversion constant.

The start of combustion (SOC) was determined, in accordance with the AVL IndiCom methodology appropriate for compression-ignition engines, as the crankshaft rotation angle at which the differential heat release rate curve dQ/dθ – after an initial negative deflection associated with the evaporation of the injected fuel dose – first returns to a value of zero again, counting backward from the maximum of this curve.

RESULTS

The crankshaft rotation angles referred to in this section relate to top dead center (TDC) of the piston of the analyzed cylinder in the compression/combustion stroke (θ = 0 °CA). Negative values denote a position before TDC, positive values a position after TDC. The angle αpw denotes the start-of-injection angle of the first pilot injection. The angle αps denotes the start-of-combustion angle. The angle α_{zs} (ignition delay angle) corresponds, in accordance with the numerical values given later in this section, to the relationship $\alpha_{zs} = \alpha_{pw} - \alpha_{ps}$.

Under the selected driving conditions, the ECU executed three fuel injection phases: the first pilot injection, designated in this paper as P1, the second pilot injection, designated as P2, and the main injection, designated as G. In the tests, only the start-of-injection angle of the first pilot injection P1 was adjusted, while the settings of the second pilot injection P2 and the main injection G were left unchanged. The results obtained for the OR90Hex10 blend were referenced to the nominal control of this blend and to diesel fuel under the nominal ECU settings.

Figure 3 presents the mean indicated pressure pi, averaged over 100 engine operating cycles. For diesel fuel under nominal control, p_i = 1.020 MPa, whereas for the OR90Hex10 blend under the nominal setting, p_i = 0.999 MPa. Changing the P1 start-of-injection angle relative to the nominal setting caused a reduction in the pi value both for advanced and retarded injection. Within the range of advancing corrections from −4 to -1 °CA, the pi values ranged from 0.951 to 0.986 MPa, while within the range of retarding corrections from +1 to +4 °CA, they ranged from 0.952 to 0.973 MPa. The highest value among the variants with a modified P1 angle was observed for the −1 °CA correction; however, it remained lower than that of the OR90Hex10 blend under nominal control. This means that changing the start-of-injection angle of the first pilot injection did not increase the mean indicated pressure.

Figure 4 presents the maximum combustion pressure Pmax. For diesel fuel under nominal control, p_{max} = 10.41 MPa; for the OR90Hex10 blend under nominal control, p_{max} = 10.74 MPa. Every change in the P1 start-of-injection angle relative to the nominal setting caused an increase in the maximum combustion pressure. For advancing corrections, the Pmax values ranged from 11.07

to 11.14 MPa, and for retarding corrections, from 11.19 to 11.27 MPa. The highest Pmax value was recorded for a P1 retardation of +4 °CA. These results indicate that the nominal P1 setting yielded the lowest maximum combustion pressure for the OR90Hex10 blend, whereas a deviation of the P1 start angle in either direction increased the mechanical load on the combustion chamber.

Figure 5 presents the maximum rate of combustion pressure rise dp/dα. For diesel fuel under nominal control, dp/dα = 0.570 MPa/°CA was obtained, whereas for the OR90Hex10 blend under nominal control, dp/dα = 0.594 MPa/°CA. Advancing the P1 start-of-injection angle increased the rate of the combustion process, particularly for the -2 and -1 °CA corrections, for which dp/dα was 0.671 and 0.711 MPa/°CA, respectively. An opposite trend was observed when retarding P1. For the +2 °CA correction, the dp/dα value decreased to 0.548 MPa/°CA, and for the +3 and +4 °CA corrections, to 0.502 and 0.504 MPa/°CA, respectively. This means that retarding the first pilot injection effectively limited the dynamics of the combustion pressure rise, with this effect being particularly pronounced for corrections greater than +2 °CA.

Figure 6 presents the mean energy released during combustion of the fuel dose. For diesel fuel under nominal control, the value was 1142.7 kJ/m³, whereas for the OR90Hex10 blend, it was 1214.2 kJ/m³. Changing the P1 start angle produced varied responses for this parameter. For advanced injection, the values ranged from 1036.6 to 1193.1 kJ/m³. On the retarded side, the highest value, 1279.1 kJ/m³, was obtained for the +2 °CA correction. This value was higher than both the result for the OR90Hex10 blend under nominal control and the result for diesel fuel. At the same time, the increase in energy released during combustion did not translate into an increase in the mean indicated pressure, which points to the significant role of combustion-process phasing relative to piston position. In other words, the two trends run in opposite directions: for the +2 °CA correction, the energy released from the fuel dose increased by approximately 5.35% relative to the nominal OR90Hex10 setting (from 1214.2 to 1279.1 kJ/m³), while pi for this correction did not increase (it fell within the range of 0.952–0.973 MPa, below the nominal value of 0.999 MPa) – the change in dose energy and the change in pi are therefore clearly decoupled from one another.

Figure 7 presents the maximum heat release rate Q_{max}. For diesel fuel under nominal control, Q_{max} = 145.2 kJ/m³·°CA was obtained, whereas for the OR90Hex10 blend under nominal control, Q_{max} = 172.8 kJ/m³·°CA. Advancing the P1 start-of-injection angle generally increased the intensity of heat release, with the highest value, 186.6 kJ/m³·°CA, obtained for the −1 °CA correction. Retarding P1, on the other hand, caused a reduction in Q_{max} relative to the nominal setting of the OR90Hex10 blend. For the +3 and +4 °CA corrections, the Q_{max} values were 155.1 and 148.2 kJ/m³·°CA, respectively, thus approaching the level obtained for diesel fuel. These results are consistent with the trend of changes in the maximum rate of pressure rise and confirm that retarding P1 limits the intensity of the initial combustion phase.

Figure 8 presents the mean start-of-combustion angle αps. For diesel fuel under nominal control, the start of combustion occurred at α_{ps} = 0.491 °CA, whereas for the OR90Hex10

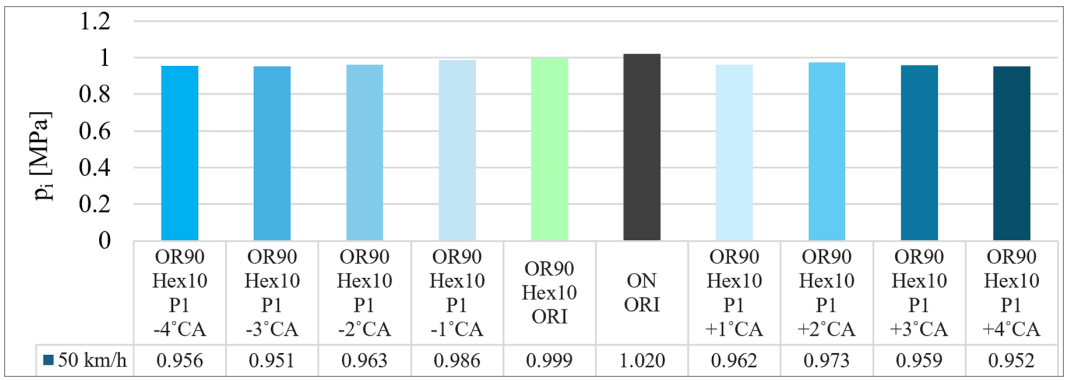


Figure 3. Mean indicated pressure, during driving on the chassis dynamometer at a speed of 50 km/h and a load torque of 50 Nm, for the selected fuels and first pilot injection control variants
The results were averaged over 100 engine operating cycles

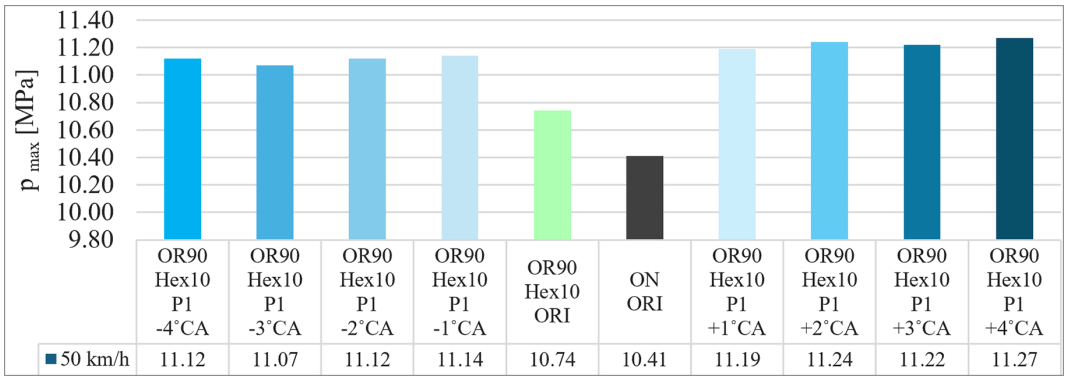


Figure 4. Maximum combustion pressure during driving on the chassis dynamometer at a speed of 50 km/h and a load torque of 50 Nm, for the selected fuels and first pilot injection control variants
The results were averaged over 100 engine operating cycles

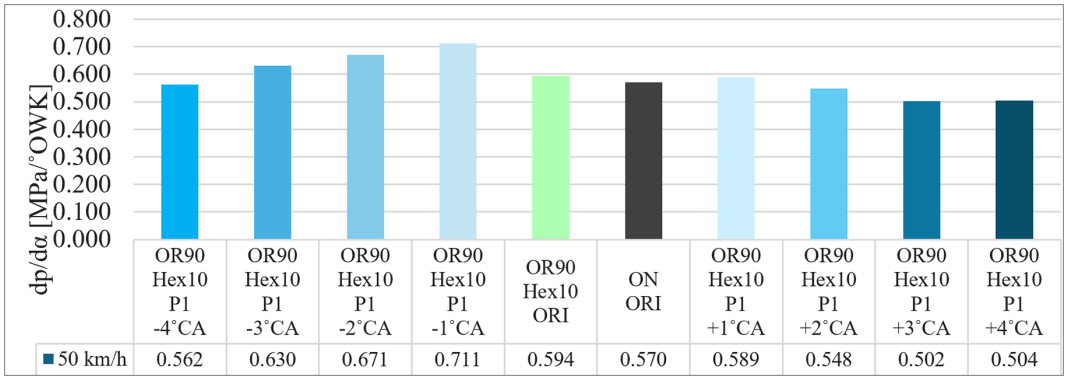


Figure 5. Maximum rate of combustion pressure rise, during driving on the chassis dynamometer at a speed of 50 km/h and a load torque of 50 Nm, for the selected fuels and first pilot injection control variants
The results were averaged over 100 engine operating cycles

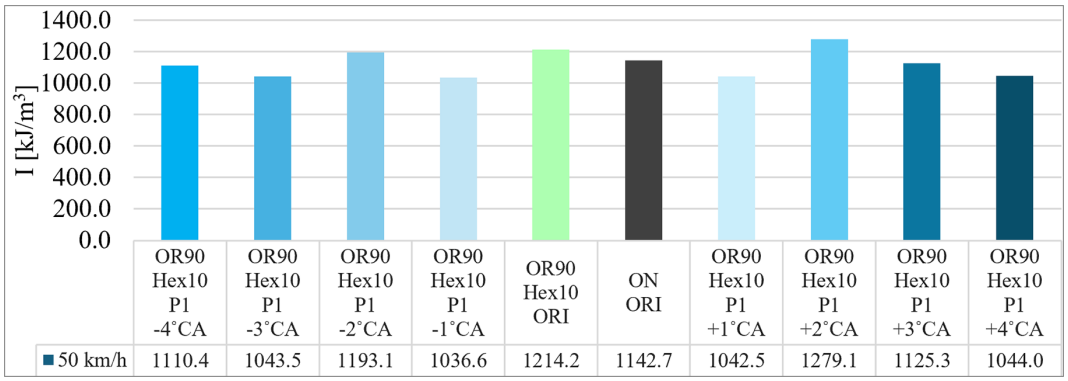


Figure 6. Mean energy released during combustion of the fuel dose, during driving on the chassis dynamometer at a speed of 50 km/h and a load torque of 50 Nm, for the selected fuels and first pilot injection control variants
The results were averaged over 100 engine operating cycles

blend under nominal control, it occurred at α_{ps} = −1.790 °CA. This means that, under the nominal ECU settings, combustion of the OR90Hex10 blend began markedly earlier than combustion of diesel fuel. Both advancing and retarding the P1 start angle caused the start of combustion to shift towards later crankshaft rotation angle values. For the retarding corrections, αps reached positive values, ranging from 1.040 to 1.760 °CA. The shift of the start of combustion beyond TDC under P1 retardation explains the observed reductions in dp/dα and Qmax.

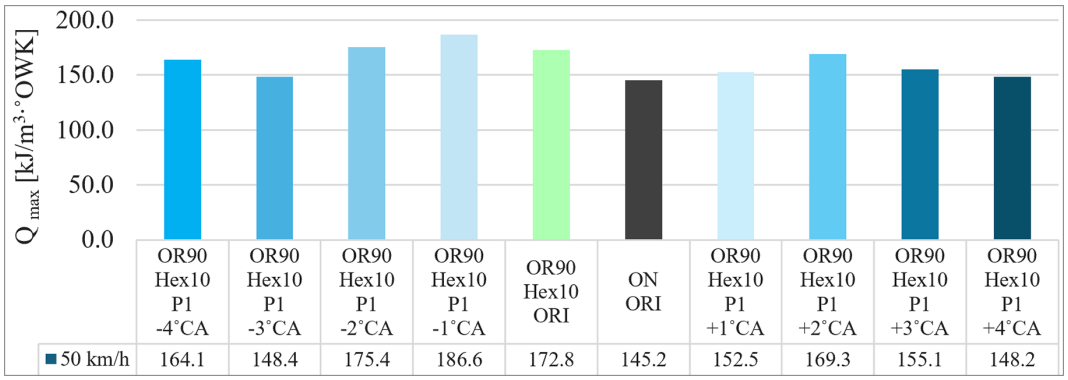


Figure 7. Maximum heat release rate, during driving on the chassis dynamometer at a speed of 50 km/h and a load torque of 50 Nm, for the selected fuels and first pilot injection control variants
The results were averaged over 100 engine operating cycles

Figure 9 presents the mean angle at which the maximum combustion pressure α pmax occurs. For the OR90Hex10 blend under nominal control, α_{pmax} was 10.39 °CA, whereas for diesel fuel under nominal control it was 11.33 °CA. Advancing P1 shifted the position of the maximum pressure towards earlier angles, with α_{pmax} equal to 9.38 °CA for the −1 °CA correction. Retarding P1, on the other hand, caused a systematic shift of the pressure maximum towards later positions, reaching 11.87 °CA for the +4 °CA correction. From the standpoint of combustion-process phasing, a favourable range was obtained with a moderate P1 retardation, particularly for the +2 °CA correction, for which the pressure maximum occurred at approximately 11.40 °CA, i.e., close to the value obtained for diesel fuel.

Figure 10 presents the mean start-of-injection angle αpw. For the OR90Hex10 blend under the nominal setting, α_{pw} = −33.99 °CA was obtained, whereas for diesel fuel under nominal control, α_{pw} = −33.89 °CA. These values indicate a practically identical start-of-injection position in the reference measurements. Advancing P1 shifted the start of injection towards earlier angles, reaching −42.29 °CA for the −4 °CA correction. On the retarding side, the α pw values gradually approached the nominal setting, reaching −34.07 °CA for the +4 °CA correction. The range of changes in the start of injection confirms the effectiveness of the introduced P1 control modification and its effect on combustion-process phasing.

Figure 11 presents the mean ignition delay angle α_{zs}. For diesel fuel under nominal control, α_{zs} = −34.38 °CA was obtained, whereas for the OR90Hex10 blend under the nominal setting, α_{zs} = −32.20 °CA. This indicates a shorter ignition delay for the OR90Hex10 blend compared with diesel fuel at the analyzed operating point. Moving the P1 start angle away from the nominal setting, in either direction, increased the absolute value of αzs, particularly on the injection-advancing side. For the −4

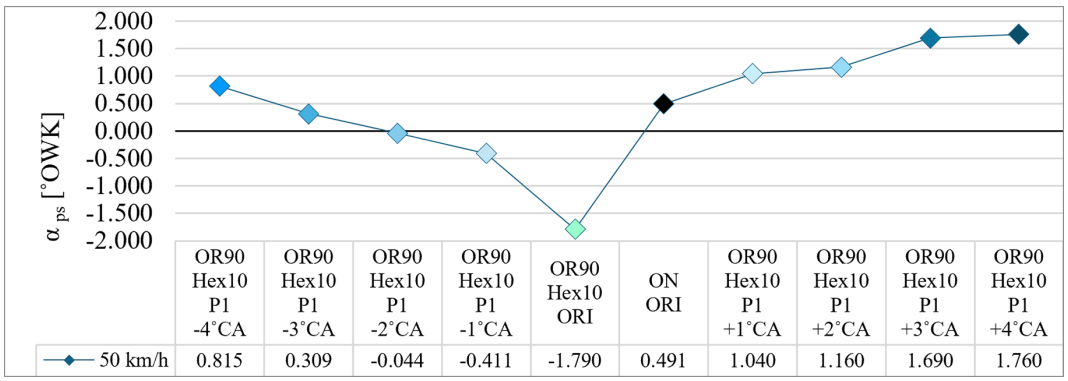


Figure 8. Mean start-of-combustion angle, during driving on the chassis dynamometer at a speed of 50 km/h and a load torque of 50 Nm, for the selected fuels and first pilot injection control variants
The results were averaged over 100 engine operating cycles

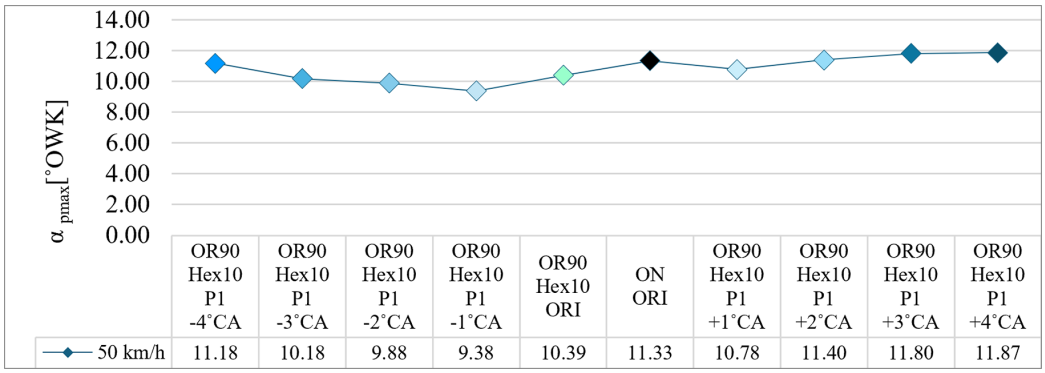


Figure 9. Mean angle at which the maximum combustion pressure occurs, during driving on the chassis dynamometer at a speed of 50 km/h and a load torque of 50 Nm, for the selected fuels and first pilot injection control variants.
The results were averaged over 100 engine operating cycles

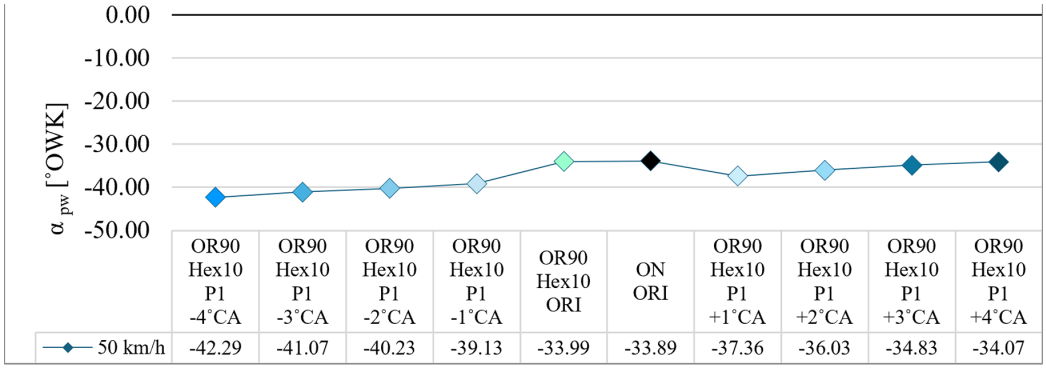


Figure 10. Mean start-of-injection angle, during driving on the chassis dynamometer at a speed of 50 km/h and a load torque of 50 Nm, for the selected fuels and first pilot injection control variants
The results were averaged over 100 engine operating cycles

°CA correction, α_{zs} = −43.10 °CA was obtained, whereas for the +4 °CA correction, α_{zs} = −35.83 °CA. The shortest ignition delay was recorded for the OR90Hex10 blend under nominal control, indicating that the original ECU settings favored the earliest onset of combustion for this fuel.

The above results, presented in Figures 3–11 as representative values for the individual variants, are averages of measurements recorded over n = 100 consecutive engine operating cycles. In order to quantitatively document the repeatability of the experiment and the cycle-to-cycle scatter

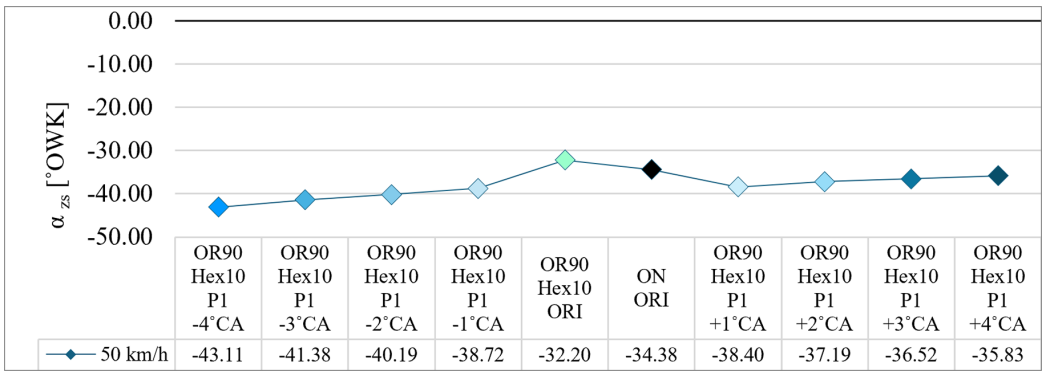


Figure 11. Mean ignition delay angle, during driving on the chassis dynamometer at a speed of 50 km/h and a load of 50 Nm, for the selected fuels and first pilot injection control variants
The results were averaged over 100 engine operating cycles

Table 4. Descriptive statistics (representative value, Std – standard deviation, CoV – coefficient of variation) of the indicated parameters, determined on the basis of n = 100 engine operating cycles for each of the analyzed variants, calculated using the AVL IndiCom software. The coefficient of variation CoV describes the cycle-to-cycle scatter of the presented value and constitutes quantitative documentation of the experiment's repeatability

Parameter/ statistic	OR90 Hex10 P1−4°CA	OR90 Hex10 P1−3°CA	OR90 Hex10 P1−2°CA	OR90 Hex10 P1−1°CA	OR90 Hex10 ORI	ON ORI	OR90 Hex10 P1+1°CA	OR90 Hex10 P1+2°CA	OR90 Hex 10 P1+3°CA	OR90 Hex10 P1+4°CA
Mean value p_i [MPa]	0.96	0.95	0.96	0.99	1.00	1.02	0.96	0.97	0.96	0.95
Std	0.04	0.05	0.05	0.04	0.02	0.03	0.05	0.05	0.05	0.04
CoV [%]	4.75	5.13	5.32	4.47	2.09	3.05	5.56	5.15	5.02	4.39
Value (max.) p_{max} [MPa]	11.1	11.1	11.1	11.1	10.7	10.4	11.2	11.2	11.2	11.3
Std	0.54	0.73	0.73	0.52	0.30	0.18	0.66	0.62	0.48	0.55
CoV [%]	5.51	7.22	7.14	4.97	2.96	1.83	6.73	6.40	5.15	5.90
Mean value $dp/d\alpha$ [MPa/°CA]	0.56	0.63	0.67	0.71	0.59	0.57	0.59	0.55	0.50	0.50
Std	0.10	0.12	0.12	0.11	0.07	0.11	0.11	0.10	0.08	0.10
CoV [%]	17.8	18.9	18.6	15.1	12.5	19.7	19.3	18.4	16.8	19.3
Mean value I [kJ/m³]	1110	1044	1193	1037	1214	1143	1042	1279	1125	1044
Std	728	688	741	700	782	726	692	794	752	698
CoV [%]	65.5	66.0	62.1	67.5	64.4	63.5	66.4	62.1	66.8	66.9
Value (max.)* Q_{max} [kJ/ m³·°CA]	164	148	175	187	173	145	152	169	155	148
Mean value α_{ps} [°CA]	0.81	0.31	-0.04	-0.41	-1.79	0.49	1.04	1.16	1.69	1.76
Std**	2.63	1.66	2.38	3.62	4.49	2.67	1.26	1.04	0.60	0.69
Mean value α_{pmax} [°CA]	11.2	10.2	9.88	9.38	10.4	11.3	10.8	11.4	11.8	11.9
Std	0.99	1.31	1.27	1.00	0.81	0.50	1.24	1.17	0.90	0.88
CoV [%]	8.87	12.9	12.9	10.6	7.78	4.42	11.5	10.3	7.66	7.45
Mean value α_{pw} [°CA]	-42.3	-41.1	-40.2	-39.1	-34.0	-33.9	-37.4	-36.0	-34.8	-34.1
Std	0.51	0.65	0.61	0.60	0.32	0.52	0.78	0.54	0.42	0.54
CoV [%]***	1.20	1.58	1.51	1.54	0.95	1.52	2.09	1.51	1.22	1.58

Note: * For Q_{max}, the presented value corresponds to the maximum of the heat release rate curve within the cycle (the Q-curve channel sampled every 1 °CA within the AVL IndiCom software's calculation window); owing to the way this channel's statistics are computed by the software (accounting for all crank-angle samples within the cycle, not only the peak value), the standard deviation and CoV are not given here, as they would not directly describe the scatter of the peak value.
** For α_{ps}, CoV was omitted because the mean value of this parameter is close to zero for some of the variants, which renders the coefficient of variation statistically unreliable; the standard deviation is given as the measure of scatter instead.
*** CoV for α_{pw} was calculated as Std/|Mean|×100%.

of the individual indicated parameters, Table 4 presents a summary of descriptive statistics (standard deviation – Std, and coefficient of variation – CoV) for all the analyzed parameters and test variants. This summary makes it possible to assess the extent to which the values presented in the figures are representative and reliable, and to identify the combustion-process stages characterized by the greatest variability between successive cycles.

An analysis of the presented coefficients of variation shows a clear differentiation in the repeatability of the individual stages of the combustion process. The start-of-injection angle αpw exhibits the lowest and most stable cycle-to-cycle variability (CoV of 0.95–2.09%), confirming the high mechanical-hydraulic repeatability of the injection system regardless of the analyzed advance angle. Similarly low scatter is observed for the

mean indicated pressure pi (CoV 2.09–5.56%) and the maximum pressure pmax (CoV 1.83–7.22%), indicating good repeatability of the total work performed within the cycle, despite variability occurring at the earlier combustion stages.

By contrast, the maximum rate of pressure rise dp/dα shows markedly higher variability (CoV 12.5–19.7%) – small differences in the timing and intensity of ignition of the fuel-air mixture translated into the dynamics of pressure rise, whereas their effect on the maximum pressure value and the total work of the cycle is already averaged out and attenuated. Similarly, the standard deviation of the start-of-combustion angle αps reaches its maximum value (4.49 °CA) for the OR90Hex10 reference (ORI) variant, at a relatively low mean value of this angle (−1.79 °CA) – this points to the greatest scatter of the ignition moment at the reference setting, while this scatter systematically decreases with increasing injection-angle advance (Std = 0.60 °CA for the +3 °CA variant), suggesting a stabilizing effect of earlier injection on the repeatability of the mixture's ignition process.

This summary confirms that the source of the observed cycle-to-cycle variability is not the injection system itself (as evidenced by the low CoV of α_{pw}), but rather the physicochemical processes preceding and accompanying the self-ignition of the rapeseed oil–n-hexane blend. Sensitivity to local conditions in the combustion chamber is transferred, to the greatest extent, to the dynamics of pressure rise (dp/dα), and, to a lesser extent, to the mean indicated pressure and maximum pressure parameters over the entire cycle.

In summary, changing the start-of-injection angle of the first pilot injection affected the phasing and dynamics of the combustion process in the OR90Hex10 blend, but did not increase the mean indicated pressure. The highest pi value for this fuel was obtained under nominal control. Advancing P1 increased the intensity of the combustion process, as evidenced by increases in dp/dα and Q_{max}, particularly for the −1°CA correction. Retarding P1, on the other hand, limited the dynamics of pressure rise and the heat release rate, shifting the start of combustion and the pressure maximum towards later crankshaft rotation angles. Among the tested variants, a particularly favorable compromise was obtained with a P1 retardation of approximately +2 °CA. In this case, a reduction in dp/dα relative to the nominal control of the OR90Hex10 blend was recorded, accompanied by a modest reduction in pi and a position of α pmax close to the value obtained for diesel fuel. These results indicate that the selection of the start-of-injection angle of the first pilot injection can primarily be used to shape combustion dynamics, rather than to increase the indicated parameters of an engine fuelled with a rapeseed oil–n-hexane blend.

CONCLUSIONS

The conducted study showed that changing the start-of-injection angle of the first pilot injection affects the combustion course of the OR90Hex10 blend, but does not improve the engine's energy parameters. At the analyzed operating point, corresponding to driving at a speed of 50 km/h and a load torque of 50 Nm, the highest mean indicated pressure pi value for the OR90Hex10 blend was obtained under nominal injection-system control. Both advancing and retarding the start-of-injection angle of the first pilot injection reduced pi, indicating that correcting this injection phase is not an effective way of increasing the indicated work.

The effect of changing P1 was revealed primarily in the dynamic combustion parameters. Advancing the start of the first pilot injection increased the maximum rate of pressure rise, dp/dα, and the maximum heat release rate, Q_{max}. This means an increase in the intensity of the combustion course and a greater share of the intense kinetic phase. From the standpoint of engine operation, this change is unfavorable, as it may increase dynamic loads and reduce the smoothness of the power unit's operation.

An opposite effect was obtained when retarding the start-of-injection angle of the first pilot injection. Shifting P1 towards later crankshaft rotation angles delayed the start of combustion and shifted the position of the maximum combustion pressure beyond TDC. This was accompanied by a reduction in dp/dα and Q_{max}, indicating a milder combustion course of the OR90Hex10 blend. This effect is particularly significant, since under nominal control, the combustion of this blend began earlier than in the case of diesel fuel.

The most favorable compromise between preserving the indicated parameters and limiting the intensity of combustion was obtained with a P1 retardation of approximately +2 °CA. For this setting, a reduction in dp/dα of approximately

7.7% relative to the nominal OR90Hex10 setting (0.594→0.548 MPa/°CA) was recorded, compared with nominal control of the OR90Hex10 blend, accompanied by a modest reduction in p_i within the range of 2.6–4.7% (0.999 MPa versus the stated range of 0.952–0.973 MPa for retarding corrections from +1 to +4 °CA). In addition, the angle at which the maximum combustion pressure occurs, αPmax = 11.40 °CA, was close to the value obtained for diesel fuel (11.33 °CA).

Further retardation of P1, despite a further reduction in dp/dα and Q_{max}, did not yield unambiguous benefits. This was because it was accompanied by a greater decrease in pi and by an increase in the maximum combustion pressure relative to the nominal setting. This means that the selection of the start-of-injection angle for the first pilot injection should be a compromise and cannot rely on the maximum possible retardation of this injection phase.

The obtained results indicate that changing the first pilot injection is not a way of increasing the engine's energy parameters during combustion of the rapeseed oil–n-hexane blend. When fuelling with OR90Hex10, retaining the nominal setting is justified when the priority is to maintain the highest pi and the lowest pmax. A moderate retardation of P1, on the order of +2 °CA, can be beneficial when the goal is to limit combustion intensity and improve engine smoothness.

Study limitations: the results were obtained for a single engine operating point (50 km/h, 50 Nm) and a single volumetric blend ratio (OR90Hex10, 90/10), with averaging over n = 100 engine operating cycles; exhaust gas composition was not the subject of this study. The conclusions should therefore be treated as preliminary and not generalized to other operating points, to other blend proportions, or to toxic exhaust emissions.

Practical implications and directions for further research: from the standpoint of ECU calibration for the OR90Hex10 blend, the results suggest retaining the nominal P1 setting when indicated energy is the priority, and considering a P1 retardation of approximately +2 °CA when the priority is to limit the dynamics of pressure rise. Further research should include extending the experiment to additional values of rotational speed and load, measuring exhaust gas composition and emissions, and conducting a systematic assessment of the effects of changes in control parameters during the individual injection phases (i.e., the second pilot injection and the main injection).

REFERENCES

1. Regulation (EC) No 715/2007 of the European Parliament and of the Council of 20 June 2007 on type approval of motor vehicles with respect to emissions from light passenger and commercial vehicles (Euro 5 and Euro 6). Off. J. EU 2007; L 171: 1–16.
2. Commission proposes new Euro 7 standards to reduce pollutant emissions from vehicles and improve air quality. European Commission Press Release, Brussels, 10 November 2022.
3. Directive (EU) 2018/2001 of the European Parliament and of the Council of 11 December 2018 on the promotion of the use of energy from renewable sources. Off. J. EU 2018; L 328: 82–209.
4. Directive (EU) 2023/2413 of the European Parliament and of the Council of 18 October 2023 amending Directive (EU) 2018/2001 as regards the promotion of energy from renewable sources. Off. J. EU 2023; L 2413: 1–77.
5. Abdullah B., Syed Muhammad S.A.F., Shokravi Z., et al. Fourth generation biofuel: A review on risks and mitigation strategies. Renew. Sustain. Energy Rev. 2019; 107: 37–50. https://doi.org/10.1016/j.rser.2019.02.018
6. Callegari A., Bolognesi S., Cecconet D., Capodaglio A. Production technologies, current role, and future prospects of biofuels feedstocks: A state-of-the-art review. Crit. Rev. Environ. Sci. Technol. 2020; 50: 384–436. https://doi.org/10.1080/10643389.2019.1629801
7. Statistics Poland (GUS). Final estimate of the main agricultural and horticultural crops in 2024. Warsaw, December 2024. Available online: stat.gov.pl (accessed: August 2026)
8. Misra R., Murthy M. Straight vegetable oils usage in a compression ignition engine — A review. Renew. Sustain. Energy Rev. 2010; 14: 3005–3013. https://doi.org/10.1016/j.rser.2010.06.010
9. Ogunwoye F.O., et al. Exploring the impact of diesel-vegetable oil blends as an alternative fuel in combustion chambers. Biofuels 2024; 15: 142–149. https://doi.org/10.1080/17597269.2024.2386482
10. Nwafor O., Rice G. Performance of rapeseed oil blends in a diesel engine. Appl. Energy 1996; 54: 345–354. https://doi.org/10.1016/0306-2619(96)00004-9
11. Labecki L., Cairns A., Xia J., Megaritis A., Zhao H., Ganippa L. Combustion and emission of rapeseed oil blends in diesel engine. Appl. Energy 2012; 95: 139–146. https://doi.org/10.1016/j.apenergy.2012.02.026
12. Yoshimoto Y., Tamaki H. Performance and emission characteristics of diesel engines fueled by rapeseed oil-gas oil blends. Trans. Jpn. Soc. Mech. Eng. Part B 2002; 68: 3191–3198. https://doi.org/10.1299/kikaib.68.3191
13. Longwic R., Sander P., Jańczuk B., Zdziennicka A., Szymczyk K. Modification of Canola Oil Physicochemical Properties by Hexane and Ethanol with

Regards of Its Application in Diesel Engine. Energies 2021; 14: 4469. https://doi.org/10.3390/en14154469

14. Longwic R., Sander P., Tatarynow D. Ecological aspects of using mixtures of canola oil with n-hexane in diesel engine. Combust. Engines 2021; 187: 48–54. https://doi.org/10.19206/ce-143245
15. Longwic R., Sander P., Zdziennicka A., et al. Combustion process of canola oil and n-hexane mixtures in dynamic diesel engine operating conditions. Appl. Sci. 2020; 10: 80. https://doi.org/10.3390/app10010080
16. Jaworski A., Kuszewski H., Longwic R., Sander P. Assessment of Self-Ignition Properties of Canola Oil–n-Hexane Blends in a Constant Volume Combustion Chamber and Compression Ignition Engine. Appl. Sci. 2023; 13: 10558. https://doi.org/10.3390/app131910558
17. Longwic R., Sander P., Jańczuk B., Zdziennicka A., Szymczyk K. Usefulness of Rapeseed Oil Modified by n-Hexane and Ethanol as Diesel Fuel. Energies 2024; 17: 6455. https://doi.org/10.3390/en17246455
18. Xu L., Bai X., Jia M., Qian Y., Qiao X., Lu X. Experimental and modeling study of liquid fuel injection and combustion in diesel engines with a common rail injection system. Appl. Energy 2018; 230: 287–304. https://doi.org/10.1016/j.apenergy.2018.08.104
19. Bittle J., Knight B., Jacobs T. The Impact of Biodiesel on Injection Timing and Pulsewidth in a Common-Rail Medium-Duty Diesel Engine. SAE Tech. Pap. 2009. https://doi.org/10.4271/2009-01-2782
20. Li Q., Backes F., Wachtmeister G. Application of canola oil operation in a diesel engine with common rail system. Fuel 2015; 159: 739–750. https://doi.org/10.1016/j.fuel.2015.06.060
21. Teoh Y.H., Masjuki H.H., How H.G., et al. Effect of two-stage injection dwell angle on engine combustion and performance characteristics of a common-rail diesel engine fueled with coconut oil methyl esters-diesel fuel blends. Fuel 2018; 234: 227–237. https://doi.org/10.1016/j.fuel.2018.07.036
22. Bo Y., Wu H., Xiao P., et al. Numerical study on the effect of multiple injection strategies on ignition processes for low-temperature diesel spray. Fuel 2022; 324: 124697. https://doi.org/10.1016/j.fuel.2022.124697
23. Fayad M.A. Influence of fuel injection timing strategies on performance, combustion, emissions and particulate matter characteristics fueled with rapeseed methyl ester in modern diesel engine. Fuel 2024; 365: 131172. https://doi.org/10.1016/j.fuel.2024.131172
24. Vallejo P., et al. Study of fuel injection and atomization processes of a diesel engine running on petroleum fuel and biofuel. E3S Web Conf. 2024; 471: 05007. https://doi.org/10.1051/e3sconf/202447105007
25. Sethin A., Oo Y.M., Thawornprasert J., Somnuk K. Effects of Blended Diesel–Biodiesel Fuel on Emissions of a Common Rail Direct Injection Diesel Engine with Different Exhaust Gas Recirculation Rates. ACS Omega 2024; 9: 20906–20918. https://doi.org/10.1021/acsomega.3c10125
26. Singh M., Kumar P., Sandhu S.S. An investigation of optimum control of injection timing/injection pressure for a multicylinder common rail direct injection engine fueled with AB20 blend. Proc. Inst. Mech. Eng. E J. Process Mech. Eng. 2024; 238: 415–426. https://doi.org/10.1177/09544089221146165
27. Gowrishankar S., Krishnasamy A. CFD analysis of combustion and emission characteristics of biodiesel under conventional and late-injection based premixed combustion conditions. Fuel 2023; 351: 129021. https://doi.org/10.1016/j.fuel.2023.129021
28. Vojtisek-Lom M., Pechout M., Mazac M. Experimental investigation of rapeseed oil combustion in a modern common-rail diesel engine. SAE Tech. Pap. 2011. https://doi.org/10.4271/2011-24-0104
29. Yoon S.K., Kim M.S., Kim H.J., Choi N.J. Effects of canola oil biodiesel fuel blends on combustion, performance, and emissions reduction in a common rail diesel engine. Energies 2014; 7: 8132–8149. https://doi.org/10.3390/en7128132
30. Turkcan A. Effects of high bioethanol proportion in the biodiesel-diesel blends in a CRDI engine. Fuel 2018; 222: 202–214. https://doi.org/10.1016/j.fuel.2018.03.032
31. Bambuleac D. Dynamical behavior of rapeseed oil and methyl ester of rapeseed oil during high-pressure injection. EPJ Web Conf. 2012; 25: 02002. https://doi.org/10.1051/epjconf/20122502002
32. Simpson T., Depcik C. Multiple Fuel Injection Strategies for Compression Ignition Engines. Energies 2022; 15: 5214. https://doi.org/10.3390/en15145214
33. Singh A.P., Agarwal A.K. Split injection strategies for biodiesel-fueled premixed charge compression ignition combustion engine – 4 Part II: Particulate studies. J. Energy Resour. Technol. 2020; 142: 102302. https://doi.org/10.1115/1.4047316
34. Pratap Singh A., Jena A., Agarwal A.K. Multiple fuel injection strategy for premixed charge compression ignition combustion engine using biodiesel blends. Int. J. Engine Res. 2023; 24: 1893–1908. https://doi.org/10.1177/14680874211066743
35. Harari P.A., Banapurmath N.R., Yaliwal V.S., et al. Effect of injection timing and injection duration of manifold injected fuels in reactivity controlled compression ignition engine operated with renewable fuels. Energies 2021; 14: 4621. https://doi.org/10.3390/en14154621
36. d'Ambrosio S., Mancarella A., Manelli A., et al. Experimental analysis on the effects of multiple injection strategies on pollutant emissions, combustion noise, and fuel consumption in a premixed charge compression ignition engine. SAE Int. J. Engines 2021; 14: 567–586. https://doi.org/10.4271/03-14-05-0037